

Chaos, coherence, and the double-slit experiment

Philippe Jacquod

*Département de Physique Théorique, Université de Genève, CH-1211 Genève 4, Switzerland
and Department of Physics, University of Arizona, 1118 E. Fourth Street, Tucson, Arizona 85721, USA*

(Received 17 June 2005; published 2 November 2005)

We investigate the influence that classical dynamics has on interference patterns in coherence experiments. We calculate the time-integrated probability current through an absorbing screen and the conductance through a doubly connected ballistic cavity, both in an Aharonov-Bohm geometry with forward scattering only. We show how interference fringes in the probability current generically disappear in the case of a chaotic system with small openings, and how they may persist in the case of an integrable cavity. Simultaneously, the typical, sample dependent amplitude of the flux-sensitive part $g(\phi)$ of the conductance survives in all cases, and becomes universal in the case of a chaotic cavity. In the presence of dephasing by fluctuations of the electric potential in one arm of the Aharonov-Bohm loop, we find an exponential damping of the flux-dependent part of the conductance, $g(\phi) \propto \exp[-\tau_L/\tau_\phi]$, in term of the traversal time τ_L through the arm and the dephasing time τ_ϕ . This extends previous works on dephasing in ballistic systems to the case of many conducting channels.

DOI: [10.1103/PhysRevE.72.056203](https://doi.org/10.1103/PhysRevE.72.056203)

PACS number(s): 05.45.Mt, 73.23.-b, 73.63.-b

I. INTRODUCTION

Ever since the inception of quantum theory, questions have been raised related to its connection to classical physics [1]. From a dynamical point of view, it is generally accepted that the Liouville and Schrödinger equations deliver the same time evolution for short enough times, $t < t_E$. In both chaotic and integrable dynamical systems, t_E goes to infinity in the semiclassical limit of large quantum numbers. In chaotic systems, however, the quantum breaktime $t_E = \lambda^{-1} |\ln \hbar_{\text{eff}}|$ does so only logarithmically slowly in the effective Planck's constant \hbar_{eff} (λ is the system's Lyapunov exponent) [2]. For $t > t_E$, the standard view is that external sources of decoherence must be invoked in order to reestablish the correspondence between quantum and classical mechanics [3–6].

Arguing that the necessity of external degrees of freedom for the quantum to classical transition remains unclear (see for instance Ref. [7]), Casati and Prosen recently performed a numerical double-slit experiment [8]. The set-up they considered is sketched in Fig. 1. One pierces two openings of width W in an otherwise closed cavity. Inside the cavity, a particle of mass $m \equiv 1$ is prepared in an initial wave packet of minimal spread in momentum. The system is considered to be semiclassical, i.e., the ratio of the linear system size and the particle's de Broglie wavelength is big $L/v = kL/2\pi \gg 1$. As time goes by, the particle leaks out of the cavity with an average decay time $\tau_d \propto L^2/(Wv) \gg \tau_f$ much larger than the time of flight $\tau_f \equiv L/v$ across the cavity, v being the particle's velocity. That is, the particle bounces many times between the cavity's boundary before exiting. One then records the integrated probability current $I(z)$ through the screen (from now on we set $\hbar \equiv 1$),

$$I(z) = \int_0^\infty dt \operatorname{Im}[\psi^*(z, y; t) \partial_y \psi(z, y; t)]_{y=y_0}. \quad (1)$$

Two different situations were considered, where the cavity was either integrable (an isosceles right triangle) or chaotic

(where the hypotenuse was replaced by a circular arc). In the integrable case, numerics showed that $I(x)$ exhibits the expected interference fringes. Those fringes were however absent in the chaotic case where $I(x)$ takes on its classical, structureless shape. These results prompted Casati and Prosen to draw two conclusions, (i) the double-slit setup provides for a “vivid and fundamental illustration of the manifestation of classical chaos in quantum mechanics,” and (ii) dynamical chaos alone (i.e., without any external source of noise, or any coupling to an external bath or environment) can produce sufficient randomization of quantum-mechanical phases resulting in a quantum to classical transition in the semiclassical limit. The reasoning path leading to conclusion (ii) is qualitatively the following. Due to the long lifetime of the particle inside the cavity, the wave packet must hit the cavity walls many times before exiting. Semiclassically, the wave packet follows many classical trajectories exiting at different times, and thus accumulating different action phases. In the regular case, because the particle's initial momentum is well defined, the action phases accumulated along all those trajectories are correlated. In the chaotic case however, the initial momentum uncertainty grows exponentially

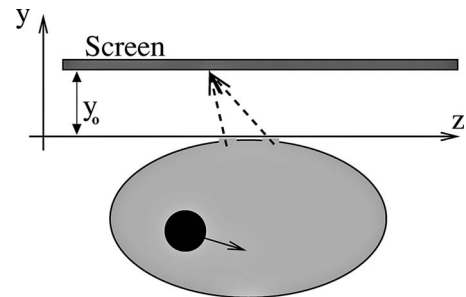


FIG. 1. (a) Double-slit setup of Ref. [8]. A cavity is pierced by two slits. A wave packet of well resolved initial momentum is prepared inside the cavity and leaks out little by little. The current through a screen is measured and integrated over time.

with time and the classical trajectories have a broad, continuous distribution of duration. Hence they acquire a random distribution of action phases. Based on this observation, Casati and Prosen concluded that this phase randomization prevents interference fringes to occur, in agreement with their numerical calculation. It is important to realize at this point that at any given point and time, the phase of the wave function is uniquely defined, and can in principle be deterministically obtained from the initial condition.

There is no controversy related to conclusion (i). Conclusion (ii) however, not only challenges the standard view according to which long-time quantum-classical correspondence requires coupling to external degrees of freedom, but must be reconciled with well-established mesoscopic physics results [9]. It is indeed well known that both transport [10–12] and thermodynamical [13–15] properties of multiply connected mesoscopic samples threaded by a magnetic flux display coherent flux-periodic oscillations of a purely quantal origin. It is doubtful that all experimentally investigated systems are integrable. From a theoretical point of view, such oscillations have been moreover predicted for disordered, diffusive samples with pointlike impurities which are arguably as good “phase-randomizers” (in the sense given above) as deterministic chaos. The even flux-harmonics (those having a period in the applied flux ϕ of $\phi_0/2n$, with n a positive integer and $\phi_0=h/e$ the flux quantum) of these oscillations even survive disorder averaging [10,14], and in the case of transport experiments “à la Sharvin and Sharvin,” the amplitude of the Aharonov-Bohm oscillations of the conductance are mostly insensitive to the amount of disorder [10]. Clearly, conductance is insensitive to the “dynamical decoherence” scenario of conclusion (ii). The purpose of this paper is to reconcile the numerical experiment of Ref. [8] with the established theoretical and experimental wisdom of mesoscopic physics, as well as to investigate dephasing in ballistic mesoscopic systems.

We will present a comparative semiclassical calculation of the outgoing probability current in the Aharonov-Bohm two-slit setup of Fig. 2(a) (similar to the setup of Ref. [8], see Fig. 1) and of the conductance in the setup of Fig. 2(b). In both cases, a cavity is connected to two intermediate left (L) and right (R) leads carrying $N_{R,L} \gg 1$ transport channels. These intermediate leads eventually merge and the loop they form is threaded by a magnetic flux ϕ . In the transport setup of Fig. 2(b), the cavity is in addition connected to a current-injecting lead carrying N_B transport channels. In the two instances, we consider ideally connected, i.e., nonreflecting leads, and will restrict ourselves to the situation where the number N_T of outgoing channels obeys $N_T \geq N_L + N_R$. One can then neglect processes where particles circulate several times around the Aharonov-Bohm loop. As but one consequence, our semiclassical treatment is fully unitary, but flux-dependent weak localization corrections are absent. Such corrections have been considered in a different ballistic setup in Ref. [16]. The setup of Fig. 2(b) in the diffusive regime has been considered in Ref. [17]. A nonunitary semiclassical treatment of the set-up of Fig. 2(b) considering backscattering due to pairs of time-reversed paths has been presented in Ref. [18].

Our conclusion is that, while there is nothing wrong with most of the reasonings and the numerical results of Ref. [8],

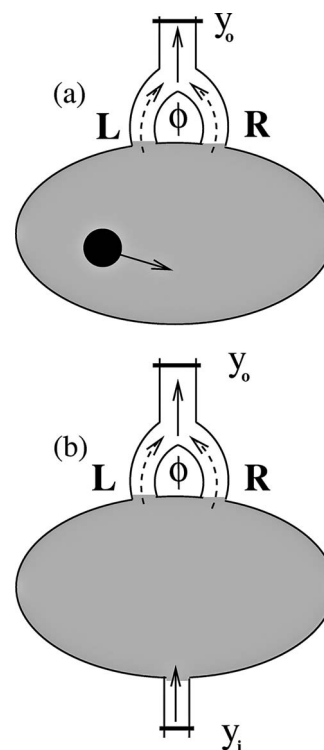


FIG. 2. (a) Double-slit setup similar to that of Ref. [8] (see Fig. 1). A cavity is pierced by two slits which are connected via an Aharonov-Bohm geometry to a single lead. A wave packet is prepared inside the cavity and leaks out little by little. The current through a cross section \mathcal{C} (located at $y=y_0$) of the outgoing lead is measured and integrated over time. (b) Transport setup. The same cavity as in (a) is connected to an additional current-injection lead. The current through \mathcal{C} is measured. Taking its ratio with the applied voltage gives the conductance.

decoherence cannot be claimed to occur when one observable does not display interference patterns, but when this is the case for all possible observables. The conductance experiment of Fig. 2(b) will be shown to exhibit sample-dependent Aharonov-Bohm oscillations in both cases of an integrable and a chaotic cavity. We will see how these oscillations disappear as dephasing is introduced. Our results support the standard wisdom according to which the quantum to classical crossover requires a coupling to external degrees of freedom.

The paper is organized as follows. In Sec. II we present a semiclassical calculation for an Aharonov-Bohm setup similar to the two-slit experiment considered in Ref. [8]. This calculation is extended to the calculation of the conductance in an Aharonov-Bohm transport setup in Sec. III. In Sec. IV we introduce dephasing by means of a fluctuating electric potential in one arm of the Aharonov-Bohm loop, and investigate the associated disappearance of flux-dependent interference fringes. In Sec. V we will summarize our findings and discuss future directions and open questions.

II. TWO-SLIT SET-UP

We first consider the Aharonov-Bohm two-slit setup of Fig. 2(a), where an initial wave packet is prepared inside the

cavity. The latter is connected to two outgoing leads carrying many transverse channels. The leads eventually merge, forming a loop threaded by a magnetic flux ϕ . Once one integrates over a cross section of the outgoing lead, the situation is fully similar to Ref. [8], with ϕ playing the role of the coordinate z along the screen (see Fig. 1). We consider an initial Gaussian wave packet $\psi_0(\mathbf{r}_1) = (\pi\nu^2)^{-d/4} \exp[i\mathbf{p}_0 \cdot (\mathbf{r}_1 - \mathbf{r}_0) - |\mathbf{r}_1 - \mathbf{r}_0|^2/2\nu^2]$, and approximate its time-evolution semiclassically by ($H = v^2/2$; remember that we set $m \equiv 1$)

$$\langle \mathbf{r} | \exp(-iHt) | \psi_0 \rangle = \int d\mathbf{r}_1 \sum_s K_s(\mathbf{r}, \mathbf{r}_1; t) \psi_0(\mathbf{r}_1), \quad (2a)$$

$$K_s^H(\mathbf{r}, \mathbf{r}_1; t) = C_s^{1/2} \exp[iS_s(\mathbf{r}, \mathbf{r}_1; t) - i\pi\mu_s/2]. \quad (2b)$$

Compared to Ref. [8], the Heisenberg uncertainty is evenly distributed between momentum and spatial coordinates in our choice of an initial state. This should not matter in a chaotic cavity, but may affect the outcome of the experiment in a regular cavity. The semiclassical propagator (2b) is expressed as a sum over classical trajectories (labeled s) connecting \mathbf{r} and \mathbf{r}_1 in the time t . For each s , the partial propagator contains the action integral $S_s^H(\mathbf{r}, \mathbf{r}_1; t)$ along s , a Maslov index μ_s , and the determinant C_s of the stability matrix. Because of the cavity openings, if \mathbf{r} in Eqs. (2) is inside the cavity, then the sum runs only over those classical trajectories that have not yet escaped at time t , whereas if \mathbf{r} lies somewhere in a lead, it runs over the trajectories that went exactly once through either of the openings to reach \mathbf{r} . Here, we are concerned with this latter case, setting $\mathbf{r} = (x, y = y_o)$ at the horizontal position x on a cross section \mathcal{C} of the outgoing lead defined by $y = y_o$ [see Fig. 2(a)]. Later on, we will integrate over x .

The semiclassical expression for the time-integrated probability current (1) is given by

$$\begin{aligned} I(x, \phi) &= \frac{v}{(\pi\nu^2)^{d/2}} \int_0^\infty dt \int d\mathbf{r}_1 \int d\mathbf{r}_2 \sum_{s(t), s'(t)} [C_s C_{s'}]^{1/2} \cos \theta_s \\ &\quad \times \exp[i\{S_s(x, y_o; \mathbf{r}_1; \phi, t) - S_{s'}(x, y_o; \mathbf{r}_2; \phi, t)\}] \\ &\quad \times \exp[i\pi(\mu_{s'} - \mu_s)/2] \exp[i\mathbf{p}_0 \cdot (\mathbf{r}_1 - \mathbf{r}_2)] \\ &\quad \times \exp[-(|\mathbf{r}_1 - \mathbf{r}_0|^2 + |\mathbf{r}_2 - \mathbf{r}_0|^2)/2\nu^2], \end{aligned} \quad (3)$$

where we used $\partial_y S_s = v_{y,s} = v \cos \theta_s$, with $v_{y,s}$ the velocity in y -direction and thus θ_s the angle of incidence, as the path s crosses \mathcal{C} at time t .

The first step in the calculation of $I(x, \phi)$ is to linearize $S_s(x, y_o; \mathbf{r}_1; \phi, t) \approx S_s(x, y_o; \mathbf{r}_0; \phi, t) - \mathbf{p}_s \cdot (\mathbf{r}_1 - \mathbf{r}_0)$, with \mathbf{p}_s the initial momentum on path s . This is justified by our choice of a narrow initial wave packet. One is then left with Gaussian integrals over $\mathbf{r}_{1,2}$. Enforcing a stationary phase condition, the dominant, classical contributions to $I(x, \phi)$ are identified as those with $s = s'$. Under our assumption of a final number of transport channels $N_T \geq N_L + N_R$ roughly equal or somehow larger than the sum of transport channels in the intermediate leads forming the Aharonov-Bohm loop, single tra-

jectories do not enclose any flux. Diagonal contributions with $s = s'$ are thus flux independent. Writing $I(x, \phi) = I_0(x) + I_\phi(x)$, one has

$$\langle I_0(x) \rangle = v(4\pi\nu^2)^{d/2} \int_0^\infty dt \sum_{s(t)} C_s \cos \theta_s \exp[-\nu^2 |\mathbf{p}_0 - \mathbf{p}_s|^2]. \quad (4)$$

The stationary phase leading to the diagonal approximation $s = s'$ is justified once one averages over an interval of energy δE which is classically small (i.e., which does not modify the trajectories) but quantum-mechanically large (i.e., such that $\delta E \cdot \tau_d \gg 1$). This is indicated by brackets in Eq. (4). The average value $\langle I_0(x) \rangle$ is calculated under the assumption that the cavity is ergodic, in particular that the wave function will eventually leak out of it completely. That is, the time-integrated current through \mathcal{C} must be equal to 1 and one has

$$\frac{2v}{\pi} \int_0^W dx \int_0^\infty dt |\psi(x, y_o; t)|^2 = 1, \quad (5)$$

where a factor $2/\pi$ originated from averaging the incidence angle on \mathcal{C} in the interval $[-\pi/2, \pi/2]$. This provides the semiclassical sum rule

$$v(4\pi\nu^2)^{d/2} \int_0^W dx \int_0^\infty dt \sum_{s(t)} C_s \exp[-\nu^2 |\mathbf{p}_0 - \mathbf{p}_s|^2] = \pi/2. \quad (6)$$

The classical time-integrated current through \mathcal{C} is then obtained as

$$\int_0^W dx \langle I_0(x) \rangle = 1. \quad (7)$$

In the limit of a wide outgoing lead, $W \gg \nu$, the probability current is ergodically distributed over \mathcal{C} so that the average current per unit length is given by $\langle I_0(x) \rangle \approx W^{-1}$.

After this warm-up calculation we turn our attention to the flux-dependent part $I_\phi(x)$. It correspond to pairs of paths s and s' in Eq. (3) exiting through different arms of the AB ring, and evidently they are not included in the diagonal approximation $s = s'$. Furthermore, no stationary phase approximation can be systematically enforced to identify them, which reflects the fact that they vanish on average. That is to say $\langle I_\phi(x) \rangle = 0$, once it is averaged over different initial conditions, a sufficiently large energy interval or an ensemble of different cavities. This is but one consequence of our choice of forward scattering processes only at the merging point of the intermediate leads.

To investigate the behavior of $I_\phi(x)$ for a given cavity and/or initial wave packet preparation, we proceed to calculate $\langle I_\phi^2(x) \rangle$, the square root of which gives the value of the flux-dependent part of $I(x)$ for a typical experimental realization. Our approach is similar in spirit to the one followed in Ref. [13] in the context of persistent currents. A similar sum rule as (6) is helpful in computing $\langle I_\phi^2(x) \rangle$, and with a little extra work we will see that $\langle I_\phi^2(x) \rangle \propto (1 - \exp[-\tau_{\text{erg}}/\tau_d])^2 (kL)^{-1} \approx (\tau_{\text{erg}}/\tau_d)^2 (kL)^{-1}$, where τ_{erg} is the ergodic time. In a chaotic cavity, it is generally given by few times the time of flight across the cavity, so that τ_{erg}/τ_d

$\propto W/L$. In the numerical experiment of Ref. [8], both the ratio of the width of the openings to the linear system size and the inverse semiclassical parameter kL are much smaller than 1, inducing the disappearance of the interference fringes.

Noting that $S_s(x, y_o; \mathbf{r}_0; \phi, t) = S_s(x, y_o; \mathbf{r}_0; t) \pm \pi \phi / \phi_0$, where the plus and minus signs correspond to trajectories going through the right and the left intermediate lead, respectively, linearizing in $\mathbf{r}_{1,2} - \mathbf{r}_0$ and performing the resulting Gaussian integrals over $\mathbf{r}_{1,2}$ as above, one has

$$I_\phi(x)I_\phi(x') = 4v^2(4\pi v^2)^d \cos^2(2\pi\phi/\phi_0) \int_0^\infty dt_1 \int_0^\infty dt_2 \sum_{s_1, s_3 \in L} \sum_{s_2, s_4 \in R} \left(\prod_{i=1}^4 C_i \right)^{1/2} \cos \theta_1 \cos \theta_4 \exp[i\{S_1(x, y_o; \mathbf{r}_0; t_1) - S_2(x, y_o; \mathbf{r}_0; t_1) - S_3(x', y_o; \mathbf{r}_0; t_2) + S_4(x', y_o; \mathbf{r}_0; t_2)\}] \exp[-v^2\{|\mathbf{p}_0 - \mathbf{p}_1|^2 + |\mathbf{p}_0 - \mathbf{p}_2|^2 + |\mathbf{p}_0 - \mathbf{p}_3|^2 + |\mathbf{p}_0 - \mathbf{p}_4|^2\}/2}], \quad (8)$$

where we shortened the notation, i.e., $\theta_i = \theta_{s_i}$, $S_i = S_{s_i}$ and so forth. It is important to keep in mind that s_1 and s_2 exit the cavity after a time t_1 , while the time of escape is t_2 for the other two trajectories s_3 and s_4 . Because trajectories exit via two different arms of the AB loop, the only stationary phase condition that can be satisfied is to set $s_1 = s_3$ and $s_2 = s_4$, which then requires to set $x = x'$ with accuracy v , and $t_1 \approx t_2$, with an accuracy given by the time $\tau^* \approx \hbar/E$ necessary for the classical ballistic flow at energy E to accumulate an action \hbar . We substitute $\int dt_1 \int dt_2 \rightarrow \tau^* \int dt_1$ to get

$$\langle I_\phi(x)I_\phi(x') \rangle \approx \delta_v(x - x') 4v^2 \tau^* (4\pi v^2)^d \cos^2(2\pi\phi/\phi_0) \int_0^\infty dt_1 \sum_{s_1 \in L} \sum_{s_2 \in R} \prod_{i=1}^2 \{C_i \cos \theta_i \exp[-v^2|\mathbf{p}_0 - \mathbf{p}_i|^2]\}, \quad (9)$$

where $\delta_v(x - x')$ enforces the condition $x = x'$ with an accuracy $\mathcal{O}(v)$. Because there is only one time integral but two summations over classical paths, one cannot use Eq. (6) directly. Assuming that the system is ergodic, which means in particular that for times long enough, $t \geq \tau_{\text{erg}} \approx \tau_f$, spatial averages equal time averages, one writes

$$\begin{aligned} \langle I_\phi^2(x) \rangle &\approx 4v^2(4\pi v^2)^d \cos^2(2\pi\phi/\phi_0) \left(\tau^* \int_0^{\tau_{\text{erg}}} dt_1 \sum_{s_1 \in L} \sum_{s_2 \in R} \prod_{i=1}^2 \{C_i \cos \theta_i \exp[-v^2|\mathbf{p}_0 - \mathbf{p}_i|^2]\} \right. \\ &\quad \left. + \int_{\tau_{\text{erg}}}^\infty dt_1 \lim_{T \rightarrow \infty} \frac{\tau^*}{T} \int_{\tau_{\text{erg}}}^T dt_2 \sum_{s_1 \in L} \sum_{s_2 \in R} \prod_{i=1}^2 \{C_i \cos \theta_i \exp[-v^2|\mathbf{p}_0 - \mathbf{p}_i|^2]\} \right). \end{aligned} \quad (10)$$

Here, the second term inside the large parentheses corresponds to trajectories $s_1(t_1)$ and $s_2(t_2)$ exiting at different times. Its contribution to the integrated current $\int dx \langle I_\phi^2(x) \rangle$ can be calculated using the sum rule (6) and making the assumption that the current is homogeneously distributed on \mathcal{C} . We find that it vanishes $\propto \lim_{T \rightarrow \infty} \tau^*/T$. The first, pre-ergodic term is highly nonuniversal and we cannot calculate it generically. We can however give an estimate to its amplitude using

$$\int_0^{\tau_{\text{erg}}} dt_1 f(t_1) g(t_1) \sim \tau_{\text{erg}}^{-1} \int_0^{\tau_{\text{erg}}} dt_1 dt_2 f(t_1) g(t_2) \sim \tau_{\text{erg}}^{-1} (1 - \exp[-\tau_{\text{erg}}/\tau_d])^2 \int_0^\infty dt_1 dt_2 f(t_1) g(t_2). \quad (11)$$

The first relation results from removing the requirement that both trajectories s_1 and s_2 in Eq. (10) exit at the same time, and to obtain the second one, we used the measure of pre-ergodic trajectories in an open chaotic cavity $\tilde{\rho}(t \leq \tau_{\text{erg}}) = \tau_d^{-1} \int_0^{\tau_{\text{erg}}} dt \exp[-t/\tau_d]$, where $\rho(t) = \tau_d^{-1} \exp[-t/\tau_d]$ is the distribution of dwell times through a chaotic system [19]. Using $\tau^*/\tau_{\text{erg}} \approx (kL)^{-1}$, and assuming again an homogeneous distribution of $I(x)$ on \mathcal{C} , we finally get the typical flux-dependent probability current as

$$\langle I_\phi^2(x) \rangle^{1/2} \sim \cos(2\pi\phi/\phi_0) (1 - \exp[-\tau_{\text{erg}}/\tau_d]) \sqrt{\frac{\tau^*}{\tau_{\text{erg}}}} \langle I_0(x) \rangle. \quad (12)$$

We believe that Eq. (12) gives an upper bound for the typical flux-dependent part of the probability current in the case of a chaotic cavity. One sees that, compared to $\langle I_0 \rangle$, $\langle I_\phi^2 \rangle^{1/2}$ is suppressed by a prefactor $(1 - \exp[-\tau_{\text{erg}}/\tau_d]) \times (kL)^{-1/2}$. In the chaotic configuration of Ref. [8], the dwell time is approximately several hundreds of times larger than the ergodic time. Together with $kL = 180$, this leads to the suppression of the flux oscillations in a given sample by a relative factor of at least $\propto (\tau_{\text{erg}}/\tau_d)(kL)^{-1/2} \leq 10^{-3}$ compared to the average current value.

While it is always risky to make generic statistical statements on regular systems, it is reasonable to expect that in this case, the pre-ergodic terms in Eq. (9) provide for most of the contributions to $\langle I_\phi^2(x) \rangle$. This is so, since for regular systems, τ_{erg} is much larger than in a chaotic system, and even

diverges in most instances, regular systems being usually not ergodic. Moreover, integrable systems exhibit periodicities and quasiperiodicities and a persistence of correlations over very large times. Starting from Eq. (8), one may thus pair trajectories either with $\tau^* \gg \hbar/E$, or even completely relaxing the restriction $|t_1 - t_2| \leq \tau^*$. One then gets the best case scenario result that

$$\langle I_\phi^2(x) \rangle_{\text{reg}}^{1/2} \sim \cos(2\pi\phi/\phi_0) \langle I_0(x) \rangle, \quad (13)$$

i.e., the flux-dependent probability current is of the same magnitude as its classical part $I_0(x)$. This is also in agreement with Ref. [8]. One should stress however that the result (13) cannot be expected to hold generically. In particular, we believe that the choice made in Ref. [8] of an initial state with narrowest momentum spread is necessary to get interference fringes satisfying (13). Presumably the choice of direction of momentum also plays a role.

To summarize this section, we have shown why the interference fringes disappear for a two-slit experiment out of a chaotic cavity. The main result of this section, Eq. (12), can be checked numerically by increasing the width W of the slits or varying kL , or both, in the numerical experiment of Ref. [8]. More qualitatively, we argued that in well chosen situations, the interference fringes have a magnitude comparable to the classical probability current if the cavity is regular.

III. TRANSPORT SETUP

We next focus on the transport setup shown in Fig. 2(b). We write the conductance as a sum of a classical and flux-dependent part, $g = g_0 + g(\phi)$. We use the semiclassical framework developed in Ref. [20]. We start from the scattering approach which relates transport properties to the system's scattering matrix [21]

$$S = \begin{pmatrix} \mathbf{r} & \mathbf{t}' \\ \mathbf{t} & \mathbf{r}' \end{pmatrix}. \quad (14)$$

For the two terminal geometry we consider, S is a 2-block by 2-block matrix, written in terms of transmission (\mathbf{t} and \mathbf{t}') and reflection (\mathbf{r} and \mathbf{r}') matrices. From S , the system's conductance is given by $g = \text{Tr}(\mathbf{t}^\dagger \mathbf{t})$ (g is expressed in units of e^2/h).

From Ref. [20], the matrix elements t_{mn} of the transmission matrix \mathbf{t} are written as

$$t_{mn} = - \sqrt{\frac{\pi\hbar}{2W_B W_T}} \sum_s \frac{\Phi_s \exp[iS_s(\mathbf{r}_B, \mathbf{r}_T; E)]}{|\cos \theta_B^{(m)} \cos \theta_T^{(n)} M_{21}^s|^{1/2}}. \quad (15)$$

The sum runs over all classical scattering trajectories entering the cavity with an angle $\pm \theta_B^{(m)}$ at any point $\mathbf{r}_B = (x, y_i)$ on a cross section C_B of the bottom lead (of geometric width W_B) and exiting it with an angle $\pm \theta_T^{(n)}$ at any point $\mathbf{r}_T = (x', y_o)$ on a cross section C_T of the top lead (of geometric width W_T). The channel indices (m, n) specify the entrance and exit angles as $\sin \theta_B^{(m)} = \pi \bar{m} / k_F W_B$ and $\sin \theta_T^{(n)} = \pi \bar{n} / k_F W_T$, $\bar{m} = \pm m$, $\bar{n} = \pm n$, while $S_s(\mathbf{r}_B, \mathbf{r}_T; E)$ gives the classical action accumulated along s . Finally M_{21}^s

$= \partial v_\perp / \partial q_\perp$ is an element of the monodromy matrix (the \perp -direction is normal to the cross sections), and there is a phase factor $\Phi_s = \text{sgn}(\bar{m}) \text{sgn}(\bar{n}) \exp[i\pi(\bar{m}x_B/W_B - \bar{n}x_T/W_T - \mu_s/2 + 1/4)]$.

All one needs to calculate the average conductance of a chaotic cavity is the following sum rule, valid in the regime of classical ergodicity [20]

$$\sum_{s(x_B, x_T; \theta_B^{(m)}, \theta_T^{(n)})} \frac{\delta(\tau - \tau_s)}{|M_{21}^s|} \simeq \frac{\cos \theta_B^{(m)} \cos \theta_T^{(n)}}{\sum(E)} \delta x_B \delta x_T \tilde{\rho}(\tau). \quad (16)$$

In contrast to Eq. (15), the sum in Eq. (16) is restricted to phase-space trajectories with a well resolved position and momentum direction on C_B and C_T , up to uncertainties $\delta x_B, \delta x_T \simeq \nu$. Here, $\Sigma(E) = 2\pi A$ gives the volume of phase space that can be visited by an ergodic particle of energy E in a cavity of area A , and $\tilde{\rho}(\tau) = \int_\tau^\infty \rho(t) dt = \exp[-\tau/\tau_d]$ gives the survival probability that a particle remains inside an open chaotic system for a time longer than, or equal to τ . The meaning of the sum rule (16) is that at any time, surviving classical trajectories have a probability to exit the cavity given by the fraction of phase-space volume covered by the leads to the total accessible volume of phase space.

From Eqs. (15) and (16), together with the relation $\tau_d = \pi A / [v(W_B + W_T)]$, it is straightforward to calculate the average conductance within the diagonal approximation. One ends up with the classical conductance

$$\langle g \rangle = \sum_{m,n} \frac{\pi\hbar}{2W_B W_T} \sum_s |\cos \theta_B^{(m)} \cos \theta_T^{(n)} M_{21}^s|^{-1} = \frac{N_B N_T}{N_B + N_T}, \quad (17)$$

where we used the relation between lead width and channel number $N = \text{Int}(k_F W / \pi)$. As was the case for the probability current, the average conductance has no flux dependence since diagonally paired trajectories do not enclose any flux.

Following the procedure we applied to $\langle I^2(\phi) \rangle$, it is straightforward to calculate the squared typical value of the flux-dependent part of the conductance $\langle g^2(\phi) \rangle$ using Eqs. (15) and (16), and $S_s(x, y_o; \mathbf{r}_0; \phi, t) = S_s(x, y_o; \mathbf{r}_0; t) \pm \pi\phi/\phi_0$. One then has

$$\begin{aligned} \langle g^2(\phi) \rangle &= \frac{16\pi^2 \hbar^2 N_B N_T}{2} \left(\int_0^\infty dt \tilde{\rho}(t) \right)^2 \cos^2(2\pi\phi/\phi_0) \\ &= 4 \frac{N_B N_T}{(N_B + N_T)^2} \cos^2(2\pi\phi/\phi_0). \end{aligned} \quad (18)$$

Compared to the square of Eq. (17), one sum over pairs of channel indices disappeared from Eq. (18) because of the stationary phase condition we enforced on each of the two pairs of orbits going through the left and right intermediate lead, respectively.

Equation (18) is the main result of this section. It shows the universality of the typical Aharonov-Bohm response of the conductance in our setup in the chaotic case. For N_B and N_T not too different from each other, $\langle g^2(\phi) \rangle$ is independent

on $\langle g \rangle$. The survival of interference fringes in the transport setup is a direct consequence of the fact that to extract the conductance, one works in energy representation. Once one writes the scattering matrix in time representation, the squared typical conductance is given by an expression similar to Eq. (3), with however two time integrals. This makes it much easier to extract stationary phase conditions, without going through the ergodicity tricks that were needed to go from Eq. (8) to Eq. (12), and explains the ease of calculation with which (18) is derived compared to its probability current counterpart of Eq. (12).

As was the case in the preceding section for the probability current, we cannot calculate $\langle g^2(\phi) \rangle$ in the integrable case without relying on assumptions which are not necessarily well controlled. In particular, there is, to the best of our knowledge, no sum rule such as (16) for regular systems. As is the case for persistent currents in ballistic systems however [22], one expects a significantly increased magnetic response, well above the chaotic value (18), because in a regular system, the dwell time distribution is not exponential, but power law $\rho(\tau) \propto \tau^{-\beta}$ [19]. In the best case scenario, one can expect a response given by the coherent sum of N responses [$N = \min(N_B, N_T)$], leading to a flux dependence of a similar amplitude as the conductance itself. Here, further numerical experiments are needed to clarify the situation.

IV. DEPHASING BY A FLUCTUATING POTENTIAL

The results (12) and (18) derived above follow from a stationary phase condition. To satisfy the latter, one relies on the exact pairing of trajectories, i.e., setting $s=s'$ where applicable, and in this way, all accumulated action phases cancel two by two. This is no longer the case in the presence of an external dephasing source. In this case, phase differences inevitably occur in pairs of contracted trajectories due to the interaction with the external source of noise at different times along the trajectory. In this section, we finally discuss this occurrence and how dephasing destroys the Aharonov-Bohm interference fringes.

Following Ref. [23], we consider that our system as a whole, including charged gates defining the cavity and the Aharonov-Bohm ring, is electrically neutral, as sketched in Fig. 3. This does not prevent local charge fluctuations to occur, which in their turn induce fluctuations of the electric potential felt by the electrons. This is a specific example of dephasing induced by an external source, in this case the electric charges on the gates defining the system, which must fluctuate to ensure that the fluctuations inside the circuit are compensated to make the whole system electrically neutral. These fluctuations result in dephasing, and without loss of generality, we will assume that they affect only electrons passing through one, say the left intermediate lead, during the traversal time $\tau_L = L_L/v$ through that lead.

We consider the case of weak coupling, where the trajectories are unaffected by the coupling to external degrees of freedom. Dephasing is introduced in our calculation via the substitution

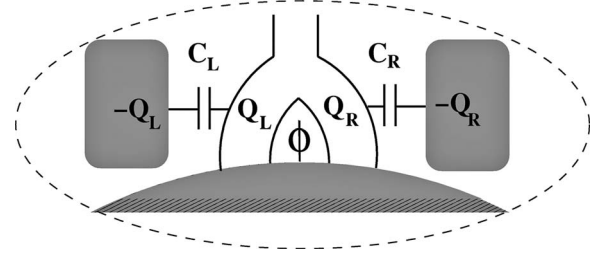


FIG. 3. Aharonov-Bohm loop capacitively coupled to external charged gates. The system as a whole (inside the dashed line; this includes the full cavity which we drew only partially) is electrically neutral, which does not prevent charge fluctuations in the arms of the loop to occur, provided they are compensated by fluctuations in the gates. The fluctuations in Q_L and Q_R induce fluctuations of the internal electric potential in the corresponding arm.

$$S_s(x, y_o; \mathbf{r}_0; t) \rightarrow S_s(x, y_o; \mathbf{r}_0; t) + \int_0^{\tau_L} dt \varphi_s(t). \quad (19)$$

Here $\varphi_s(t)$ gives the additional action phase accumulated by an electron traveling on path s and interacting with the dephasing source at time t .

Using the central limit theorem, Eqs. (12) and (18) must then be multiplied by

$$\exp\left(-\int_0^{\tau_L} dt_1 \int_0^{\tau_L} dt_2 \langle \varphi_s(t_1) \varphi_s(t_2) \rangle_s / 2\right), \quad (20)$$

where $\langle \dots \rangle_s$ denotes an average over the distribution of phases on different classical trajectories. Further assuming an exponential decay of the phase correlator $\langle \varphi_s(t_1) \varphi_s(t_2) \rangle_s = \langle \varphi_s^2(0) \rangle_s \exp[-|t_1 - t_2|/\tau_c]$, one gets, in the limit $\tau_c \ll \tau_L$, an exponential suppression of the flux response

$$\langle g^2(\phi) \rangle = \frac{N_B N_T}{(N_B + N_T)^2} \cos^2(2\pi\phi/\phi_0) e^{-\tau_L/\tau_c}, \quad (21)$$

where $\tau_c^{-1} = 2\tau_c \langle \varphi_s^2(0) \rangle_s$. In the limit of Nyquist noise, a self-consistent calculation of the phase correlator has been performed in Ref. [23], within the one-potential approximation, i.e., assuming that the fluctuations of the electric potential are spatially homogeneous inside one arm. A linear temperature dependence of the dephasing rate was obtained, which in our case translates into

$$\tau_c^{-1} = 2\tau_c \langle \varphi_s^2(0) \rangle_s = 8\pi\gamma_L^2 k_B T / N_L. \quad (22)$$

Here, $\gamma_L \ll 1$ stands for the ratio between the electrochemical and the electrical capacitance of the left arm [23]. In the weak coupling limit we are considering, one has $\gamma_L \approx 1$. Both the exponential damping of the Aharonov-Bohm flux and the linear temperature dependence of the dephasing rate are in agreement with the experimental results of Ref. [24] on Aharonov-Bohm conductance oscillations in few-channel ballistic systems. Our results (20)–(22) extend those of Ref. [23] to the many-channel case.

As a side remark, we note that in the other limit $\tau_c \gg \tau_L$, one gets a Gaussian suppression of the flux response in the traversal time τ_L ,

$$\langle g^2(\phi) \rangle = \frac{N_B N_T}{(N_B + N_T)^2} \cos^2(2\pi\phi/\phi_0) e^{-\tau_L^2/\tau_\varphi\tau_c}, \quad (23)$$

with the same dephasing time as above. This Gaussian damping has not been obtained previously. Indeed, previous works always assumed δ -correlated phases, $\langle \varphi_s(t_1)\varphi_s(t_2) \rangle_s \propto \delta(t_1 - t_2)$, meaning $\tau_c/\tau_L \rightarrow 0$.

To close this section, we remark that the same dephasing behavior will occur in regular systems as long as the phase correlator decays fast enough. While in that case, an exponential decay is not at all obvious from a dynamical point of view, we stress that, in the limit of long traversal times $\tau_L \gg \tau_c$, the minimal requirement for an exponential damping as in Eq. (21) is a power law decay of the phase correlator $\langle \varphi(t_1)\varphi(t_2) \rangle = \langle \varphi(0)\varphi(0) \rangle [\tau_c/(\tau_c + |t_1 - t_2|)]^\alpha$ with $\alpha > 1$.

V. CONCLUSION

We have presented a semiclassical calculation of the flux dependence of the probability current and the conductance in two distinct Aharonov-Bohm setups (see Fig. 2). We have shown how the interference fringes in the probability current disappear in chaotic systems in the case of cavities with large dwell times, whereas they may persist in the case of a regular cavity. This is in agreement with and sheds light on the numerical results of Ref. [8]. Simultaneously, we showed how the situation is completely different in the transport setup, where the flux response of the conductance becomes universal in the chaotic case. This universality is lost in the case of integrable cavities, where we conjectured that the flux response may be of the same order as the conductance itself.

In the transport setup, we argued that dephasing from external degrees of freedom is necessary to wash out the flux-periodic interference fringes in the conductance. We introduced dephasing in a similar way as in Refs. [16,23] and found that flux-dependent interference fringes in the conductance vanish exponentially, $\exp[-\tau_L/\tau_\varphi]$. Both this exponential damping and the linear temperature dependence of the

dephasing time (22) are in agreement with transport experiments on ballistic Aharonov-Bohm systems [24]. Our results confirm the standard view that external sources of decoherence are generally required to induce a complete quantum-classical correspondence.

Our semiclassical treatment extends the results of Refs. [16,23] to the many-channel case. Still, the dephasing behavior of Eqs. (20) and (21) relies on the one-potential approximation giving the linear temperature dependence of the phase correlator, Eq. (22). Because Ref. [8] considered the other limit of subwavelength slits, it is likely that diffraction effects play a role there that was neglected here. However, we do not expect diffraction to alter the situation qualitatively.

One of our motivations was to reconcile the results of Ref. [8] with well-known mesoscopic physics theoretical and experimental results. That is why we deliberately made the hypothesis of forward scattering only, that particles entering one of the intermediate leads (indicated by L and R in Fig. 2) are transferred to the outgoing lead with probability one. This is justified in the case where the latter lead is somehow wider than the two intermediate leads together, $N_T \gtrsim N_R + N_L$. It would be interesting to lift that hypothesis, and consider the emergence of higher flux harmonics and of flux-dependent weak localization corrections to the average conductance, and the influence that dephasing has on them. We expect that the presence of weak-localization corrections would result in the usual Lorentzian damping of the amplitude of Aharonov-Bohm interference fringes in the disorder-averaged conductance (as opposed to the typical conductance calculated here). Further investigations are however necessary to confirm this.

ACKNOWLEDGMENTS

This work has been supported by the Swiss National Science Foundation. It is a pleasure to thank M. Büttiker for drawing our attention to Ref. [8] and for several interesting discussions and comments.

-
- [1] *Quantum Theory and Quantum Measurement*, edited by J. A. Wheeler and W. H. Zurek (Princeton University Press, Princeton, NJ, 1983).
- [2] G. P. Berman and G. M. Zaslavsky, *Physica A* **91**, 450 (1978).
- [3] B. L. Altshuler, A. G. Aronov, and D. Khmel'nitskii, *J. Phys. C* **15**, 7367 (1982).
- [4] E. Joos and H. D. Zeh, *Z. Phys. B: Condens. Matter* **59**, 223 (1985).
- [5] A. O. Caldeira and A. J. Leggett, *Phys. Rev. A* **31**, 1059 (1985).
- [6] M. Büttiker, *Phys. Rev. B* **33**, 3020 (1986).
- [7] G. Casati and B. V. Chirikov, *Physica D* **86**, 220 (1995).
- [8] G. Casati and T. Prosen, *Phys. Rev. A* **72**, 032111 (2005).
- [9] Y. Imry, *Introduction to Mesoscopic Physics* (Oxford University Press, Oxford, 1997); E. Akkermans and G. Montambaux, *Physique Mésooscopique des Electrons et des Photons* (EDP Sciences, New York, 2004).
- [10] A. G. Aronov and Yu. V. Sharvin, *Rev. Mod. Phys.* **59**, 755 (1987).
- [11] R. A. Webb, S. Washburn, C. P. Umbach, and R. B. Laibowitz, *Phys. Rev. Lett.* **54**, 2696 (1985).
- [12] A. Yacoby, M. Heiblum, D. Mahalu, and H. Shtrikman, *Phys. Rev. Lett.* **74**, 4047 (1995).
- [13] H.-F. Cheung, E. K. Riedel, and Y. Gefen, *Phys. Rev. Lett.* **62**, 587 (1989).
- [14] F. von Oppen and E. K. Riedel, *Phys. Rev. Lett.* **66**, 84 (1991); B. L. Altshuler, Y. Gefen, and Y. Imry, *ibid.* **66**, 88 (1991).
- [15] L. P. Lévy, G. Dolan, J. Dunsmuir, and H. Bouchiat, *Phys. Rev. Lett.* **64**, 2074 (1990); V. Chandrasekhar, R. A. Webb, M. J. Brady, M. B. Ketchen, W. J. Gallagher, and A. Kleinsasser, *ibid.* **67**, 3578 (1991).
- [16] G. Seelig, S. Pilgram, and M. Büttiker, *Turk. J. Phys.* **27**, 331

- (2003).
- [17] T. Ludwig and A. D. Mirlin, Phys. Rev. B **69**, 193306 (2004); C. Texier and G. Montambaux, Phys. Rev. B **72**, 115327 (2005).
- [18] S. Kawabata and K. Nakamura, J. Phys. Soc. Jpn. **65**, 3708 (1996); Phys. Rev. B **57**, 6282 (1998).
- [19] W. Bauer and G. F. Bertsch, Phys. Rev. Lett. **65**, 2213 (1990).
- [20] H. U. Baranger, R. A. Jalabert, and A. D. Stone, Phys. Rev. Lett. **70**, 3876 (1993); K. Richter and M. Sieber, *ibid.* **89**, 206801 (2002).
- [21] R. Landauer, Philos. Mag. **21**, 863 (1970); M. Büttiker, Phys. Rev. Lett. **57**, 1761 (1986).
- [22] F. von Oppen and E. K. Riedel, Phys. Rev. B **48**, 9170 (1993).
- [23] G. Seelig and M. Büttiker, Phys. Rev. B **64**, 245313 (2001).
- [24] A. E. Hansen, A. Kristensen, S. Pedersen, C. B. Sørensen, and P. E. Lindelof, Phys. Rev. B **64**, 045327 (2001); K. Kobayashi, H. Aikawa, S. Katsumoto, and Y. Iye, J. Phys. Soc. Jpn. **71**, 2094 (2002).